Thermally Responsive Interactions between the PEG and PNIPAAm Grafts Attached to the PAAc Backbone and the Corresponding Structural Changes of Polymeric Micelles in Water

Yuan-Hung Hsu,[†] Wen-Hsuan Chiang,[†] Chien-Hsien Chen,[†] Chorng-Shyan Chern,[‡] and Hsin-Cheng Chiu[†,*]

Department of Chemical Engineering, National Chung Hsing University, Taichung 402, Taiwan, and Department of Chemical Engineering, National Taiwan University of Science and Technology, Taipei 106, Taiwan

Received June 17, 2005; Revised Manuscript Received August 23, 2005

ABSTRACT: Graft copolymers comprising poly(acrylic acid) (PAAc) as the backbone and poly(*N*-isopropylacrylamide) (PNIPAAm) and monomethoxy poly(ethylene glycol) (mPEG) as the grafts were prepared and characterized. These copolymers with the AAc residues in the negatively charged state underwent self-assembling into large polymeric aggregates in water in the range 32−35 °C due to the formation of the multicore structure (comprising several solidlike hydrophobic PNIPAAm cores surrounded by the liquidlike interfacial layers) and the intercore PEG connections. These rather labile intercore PEG connections were partially destroyed due to the continual dehydration and solidification of the liquidlike interfacial layers with increasing temperature, thereby leading to fragmentation of the original aggregates into smaller particles with the more distinct core/shell structure. The final particle size was virtually governed by the structure of the hydrophobic PNIPAAm microdomains in response to the effects of the PNIPAAm concentration and temperature on the intercore PEG connections.

Introduction

Amphiphilic block and graft copolymers have received growing interest, especially in their supramolecular structure formed as a result of self-assembling into micelles in the aqueous phase.[1−19] The unique supramolecular arrangements in the particulate form shows great potential in applications of biomedical and biochemical fields (e.g., drug delivery systems, biosensing, and protein separation and immobilization). Particular attention has been paid to the phase transition behavior of the poly(*N*-isopropylacrylamide) (PNIPAAm) based copolymers and the structural response of the polymeric micelles to temperature owing to the thermally controllable coil-to-globule transition in a reversible manner.[9−19] Although the colloidal properties varied with the molecular architecture of the PNIPAAm based copolymers, the hydrodynamic volume of micelles was reported to be relatively insensitive to changes in temperature once the compact structure of the hydrophobic core was attained.[9,19,20] However, the extent of physical entanglement of polymeric chains varies with the heating rates, especially in the temperature range around the phase transition of the PNIPAAm based copolymers. This would lead to the changes in the structure and size of polymeric micelles.[11,15,19] The slow heating rate around the phase transition temperature usually resulted in more extensive aggregation of polymeric micelles. On the other hand, viscosity and neutron scattering measurements of the aqueous solutions of the PNIPAAm grafted copolymers indicated that the particle structure was significantly affected by the thermally induced physical cross-linking among the PNIPAAm associated microdomains.[13,14] The intramolecular bridging among the hydrophobic PNIPAAm microdomains is expected to occur more easily for the PNIPAAm grafted copolymers compared to the PNIPAAm block copolymers or graft copolymers with PNIPAAm as the backbone. However, very few studies were concerned with the interactions of the hydrophobic microdomains of the PNIPAAm grafts with the second polymer grafts attached to the copolymer backbone when temperature was varied. Poly(ethylene glycol) (PEG) is undoubtedly the best choice for the second graft due to its unique amphiphilic property and the steric stabilization effect available for preventing particles from aggregation in aqueous solution.

In this study, the graft copolymers comprising monomeric units of acrylic acid (AAc) as the backbone and PNIPAAm and mPEG as the grafts were prepared and characterized. The supramolecular architecture of the polymeric micelles as a function of temperature was determined mainly by the variable temperature ^{1}H NMR. It is also interesting to study the role of the PEG grafts in regulating the particle size and morphology at different temperature. Therefore, the AAc residues of the copolymer backbone were kept in the negatively charged state in order to restrict the interactions of PNIPAAm grafts only with PEG at high temperature. In addition, because of the relatively high contents of PEG grafts and ionized AAc residues in the graft copolymer, a polymer concentration of 10 mg/mL or higher required to obtain particles with a more distinct core/shell structure at high temperature was thus exploited extensively.

Experimental Section

Polymer Synthesis. Poly(*N*-acryloxysuccinimide) (PNAS) was obtained by free radical polymerization of NAS in DMF. NAS was prepared by esterification of *N*-hydroxysuccinimide with acryloyl chloride,[21] and the structure and purity of the product were confirmed by NMR, FTIR, and elemental analy-

[†] National Chung Hsing University.
[‡] National Taiwan University of Science and Technology.
* To whom correspondence should be addressed: Fax 886-422854734; Tel 886-422852636; e-mail hcchiu@dragon.nchu.edu.tw.

10.1021/ma0512713 CCC: $30.25
Published on Web 10/20/2005

Scheme 1. Schematic Illustration of the Synthesis and Chemical Structure of the Graft Copolymers

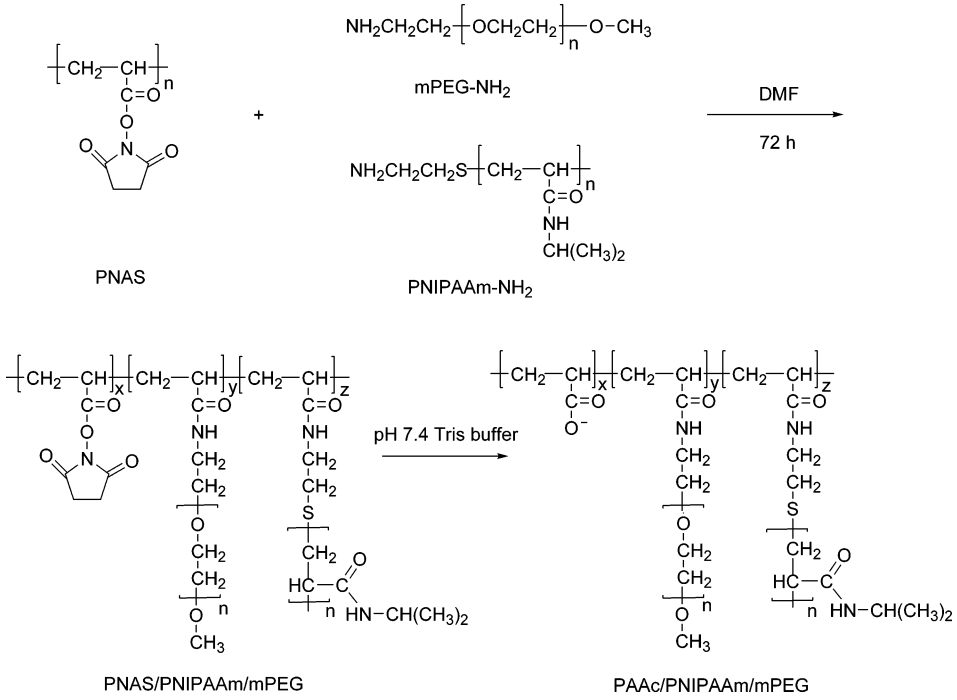

sis. To a solution of NAS (15 g) in DMF (90 mL), 2,2′-azobis-(isobutyronitrile) (AIBN) (0.6 g) as an initiator was added at 60 °C under vigorous stirring, and the reaction was carried out for 15 h under a nitrogen atmosphere. PNAS was purified and collected by precipitation from acetone twice and dried in vacuo. The chemical structure was confirmed by FTIR and ^{1}H NMR separately. Prior to molecular weight measurements, PNAS was subjected to thorough hydrolysis in tris buffer (pH 7.4), followed by dialysis (Spectra/Por MWCO 6000−8000) against deionized water and lyophilization. The average molecule weight of the resulting PAAc was determined by size exclusion chromatography (SEC) (Agilent 1100, PL Aquagel-OH columns in series GF083: separation range 100−30K; GF084: 10K−200K; and GF086: 200K−10M, calibrated with poly(sodium acrylate) standards of known molecular weights with narrow molecular weight distributions (Polymer Laboratories); eluent: tris buffer 0.1 M, pH 7.4; flow rate: 1 mL/min; RI detector (Agilent 1100)).

The grafting reaction involved the preparation of aminated semitelechelic PNIPAAm by radical polymerization of NIPAAm in methanol, using AIBN as the initiator and 2-aminoethanethiol hydrochloride as the chain transfer agent.[22] The number-average molecule weight was determined to be 2700 g/mol by the amino end-group titration with trinitrobenzenesulfonic acid (TNBS). Monoamino-mPEG (2000 g/mol) was prepared according to the method reported elsewhere.[23] The TNBS assay showed that the amination efficiency of mPEG was ca. 95%. To solutions of PNAS (3 g each, 10% w/v) in DMF, semitelechelic PNIPAAm (10 mol % (referred to as copolymer **A**) and 20 mol % (**B**) with respect to the NAS residues) and mPEG (10 mol %) in DMF (10% w/v) were added separately. The reaction was carried out at 25 °C under stirring for 72 h. The unreacted NAS residues in the graft copolymers were hydrolyzed into to AAc units by addition of excess tris buffer (0.1 M and pH 7.4). The solution was subjected to dialysis (Spectra/Por MWCO 6000−8000) against deionized water primarily for removing DMF and NHS, followed by diafiltration (Millipore, Labscale TFF System equipped with Pellicon XL membrane Biomax-30 MWCO: 30 000) in the absence of DMF to eliminate more efficiently the unconjugated PNIPAAm and mPEG. The graft copolymers were then dissolved in deionized water, and pH was adjusted to 6.7−7.0 by dilute NaOH solution and maintained for 2 h. Subsequently, the polymers were collected by lyophilization. The purity of the copolymers was confirmed by SEC as aforementioned. The synthetic route and the chemical structure of the graft copolymers are illustrated in Scheme 1. Determination of the graft copolymer compositions was carried out by ^{1}H NMR in $CDCl_3$ at 20 °C. During the NMR measurement, DMF in a sealed capillary was placed coaxially in the sample tubes as an external standard for establishing the calibration curve and determining the composition ratios of the graft copolymers. The external reference exhibits its feature proton signals at δ 2.9 and 3.1 ppm from the dimethyl group and at 8.1 ppm from the formyl group, with the integral ratios at 3:3:1. Calibration was obtained from the relative signal integrals of mPEG at δ 3.6 ppm with eight concentrations in $CDCl_3$ with respect to the signal integral of DMF at δ 8.1 ppm. Figure 1 illustrates a representative ^{1}H NMR spectrum of copolymer **B** (10.0 mg/mL) in $CDCl_3$ at ambient temperature. The composition of the graft copolymer was determined by the mass balance based on the calibration curve and the signal integrals of mPEG at 3.6 ppm and PNIPAAm grafts at 1.1 ppm. The recipes, compositions, and average molecular weights of the graft copolymers are listed in Table 1.

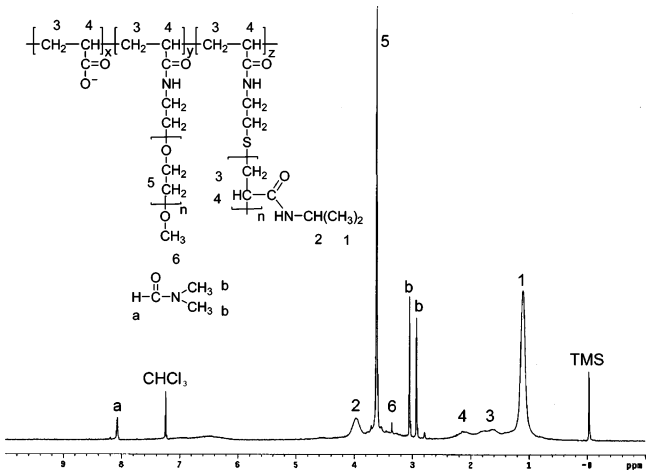

Figure 1. ^{1}H NMR spectrum of copolymer **B** (10.0 mg/mL) in $CDCl_3$ at 20 °C. The assignment of the feature signals of the copolymer and the external standard (DMF) in relation to the chemical structure is also included.

Table 1. Recipes, Composition, and Structural Characterization

	reaction feeds (mol %) NAS/mPEG/PNIPAAm	composition ratios[a] (mol %) AAc/mPEG/PNIPAAm	grafting efficiency (%) PEG	grafting efficiency (%) PNIPAAm	M_w[b] ($\times 10^{-4}$) (g/mol)	CP[c] (°C)	CAC[d] ($\times 10^{-5}$) (g/mL)
A	100/10/10	85.9/6.9/7.2	69	72	11.2	34.1	5.45
B	100/10/20	78.5/6.9/14.6	69	73	16.7	33.5	4.58

[a] Calculated by the ^{1}H NMR measurements in $CDCl_3$. [b] Obtained by theoretical calculation: M_w(PAAc) + number of mPEG grafts × 2000 (M_w of mPEG) + number of PNIPAAm grafts × 2700 (M_w of PNIPAAm). [c] CP: cloud point that was determined by the transmittance measurements of the aqueous polymer solutions (10.0 mg/mL) at 50% reduction. [d] CAC: critical aggregation concentration that was determined by the fluorescence intensity ratio I_3/I_1 of pyrene in the aqueous polymer solutions with varying concentrations at 37 °C.

Structural Characterization of Micelles. The aqueous polymer concentration of 10.0 mg/mL was used, unless stated otherwise. The temperature was programmed to increase from 20 to 60 °C, but with an interval of 1.0 °C for 30 min in the range from 30 to 35 °C. This heating approach was referred to as the slow heating in the literature.[11,15,19] Fluorescence experiments were performed by measuring changes in the ratio of the peak height of the third vibronic band at 385.5 nm to the first at 373.5 nm of the emission spectra of pyrene in aqueous polymer solutions (I_3/I_1) as a function of temperature.[24] The pyrene concentration was kept at 6.0×10^{-7} M. The excitation was induced at 336 nm, and the emission spectra in the range from 350 to 500 nm were recorded on a Hitachi F-2500 fluorescence spectrometer equipped with a thermostat cell unit.

The hydrodynamic diameter (D_h) of micelles in deionized water was determined by the Brookhaven 90 plus particle size analyzer (He−Ne laser 15 mW, $\lambda = 678$ nm) at a fixed angle of 90°. Prior to measurement, the sample was passed through a 0.2 μm filter at 20 °C and then equilibrated at each preset temperature for 30 min. In some experiments, the particle size was also determined immediately after the sample was subjected to mild mixing at each preset temperature. The mild mixing herein is referred to as the reciprocal shaking at a speed of 45 rpm for 30 s.

^{1}H NMR spectra of the graft copolymers in D_2O were obtained from a Varian Unity Inova-600 at 600 MHz in the absence of the sample spinning. The pulse width of 4.9 μs with a relaxation delay of 2 s was utilized. The identical DMF external reference in capillary as aforementioned was used repeatedly. The proton signal of DMF at δ 8.1 ppm was utilized as the reference for the assignment and evaluation of the signal position and integral, respectively, compared to those in $CDCl_3$ at ambient temperature. The standard inversion−recovery pulse sequence (180°−τ−90°) was employed to determine the spin−lattice relaxation times (T_1) of the feature signals of the copolymers **A** and **B** (Varian Unity Inova-600 at 600 MHz). In each measurement, 13−15 variable delays were used, and the waiting period was adjusted at least 5 times larger than the expected relaxation time. T_1 was then calculated using a nonlinear least-squares fitting routine of the spectrometer.[25]

Deviation in the interactions of the graft copolymers with water molecules was quantitatively evaluated in terms of the volumetric (or density) change of these copolymers in water. The density measurement was conducted with a U-tube vibrating densimeter (Anton Paar DMA-5000), controlled within $\pm 5 \times 10^{-6}$ g cm^{-3} and ±0.001 °C. The effect of changes in viscosity with temperature was eliminated by the autocorrelation function. Prior to the density measurements, the densimeter was calibrated at 20 °C, using air and deionized water as the reference fluids. The densities of polymer aqueous solutions ($\rho_{solution}$) and water (ρ_{H_2O}) were recorded at different temperatures. On the basis of the assumption of the volume additivity, the density of the polymer aqueous solutions at each corresponding temperature determined experimentally can be expressed as follows:

$$\rho_{solution}(T) = \frac{M_{solution}}{V_{solution}(T)} = \frac{M_{polymer} + M_{H_2O}}{V_{polymer}(T) + V_{H_2O}(T)} \quad (1)$$

Here $M_{solution}$, $M_{polymer}$, and M_{H_2O} are the masses of the aqueous polymer solution, the graft copolymer, and water in the sample tube, and $V_{solution}(T)$, $V_{polymer}(T)$, and $V_{H_2O}(T)$ are their volumes at each corresponding temperature, respectively. By rearrangement of eq 1 with the relationship among M, V, and ρ, the apparent density (ρ_m) of the graft copolymers at each temperature was obtained according to the following equation:

$$\rho_m(T) = \frac{\rho_{H_2O}(T)\rho_{solution}(T)M_{polymer}}{\rho_{H_2O}(T)(M_{polymer} + M_{H_2O}) - \rho_{solution}(T)M_{H_2O}} \quad (2)$$

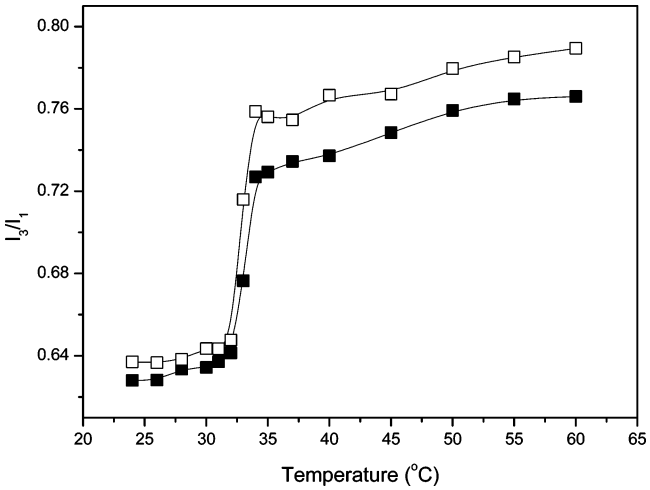

Figure 2. Effect of temperature on the fluorescence intensity ratio I_3/I_1 of pyrene in the aqueous solutions of copolymers **A** (■) and **B** (□) (10.0 mg/mL).

Results and Discussion

Graft copolymers comprising the monomeric units of AAc as the copolymer backbone and PNIPAAm and mPEG as the grafts were obtained from the partial aminolysis of PNAS with aminated semitelechelic PNIPAAm and mPEG, followed by thorough hydrolysis of the remaining NAS into the AAc residues along the backbone (Scheme 1). Both aminated semitelechelic PNIPAAm and mPEG of average molecular weights 2700 and 2000 g/mol, respectively, were used throughout this study. The SEC results indicated that the weight-average molecular weight and polydispersity of the corresponding PAAc after complete hydrolysis of the PNAS precursor were ca. 20 000 g/mol and 1.8, respectively. The composition data of the two copolymers **A** and **B** that are different only in the PNIPAAm contents are shown in Table 1. The recipes and some fundamental characterization results are also included in Table 1.

A dramatic change in the fluorescence intensity ratios (I_3/I_1) was observed in the range 32−34 °C (Figure 2). The results are in good agreement with the cloud points of the graft copolymers listed in Table 1. Since the value of I_3/I_1 represents a quantitative measure of the nonpolarity nature of the microenvironment where most hydrophobic pyrene molecules reside, the trend observed

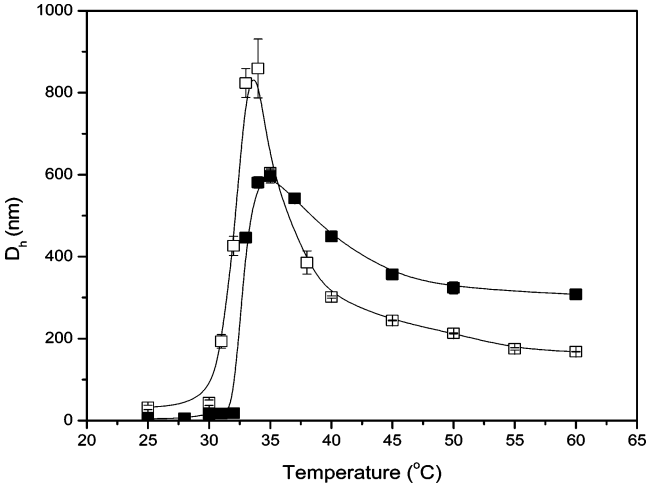

Figure 3. Variation of the *z*-average hydrodynamic diameter (D_h) of copolymers **A** (■) and **B** (□) (10.0 mg/mL) in aqueous solutions with temperature in the absence of agitation.

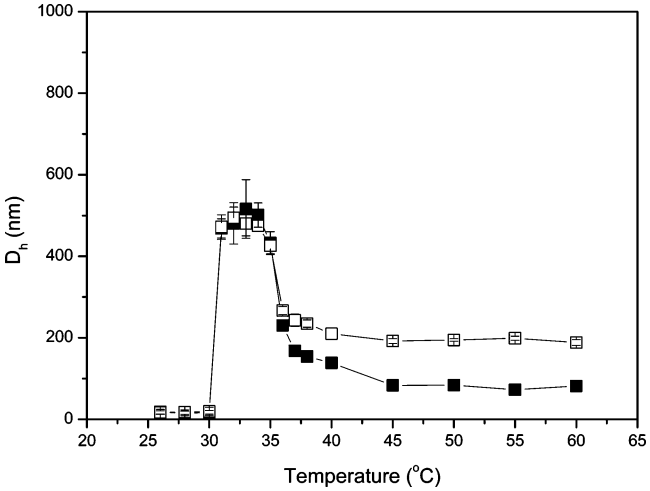

Figure 4. Variation of the *z*-average hydrodynamic diameter (D_h) of copolymers **A** (■) and **B** (□) (10.0 mg/mL) in aqueous solutions with temperature under mild agitation.

in Figure 2 is attributed to the structural response of the copolymers to the increased temperature. In this temperature range, the copolymers underwent a coil-to-globule transition in the conformation of PNIPAAm grafts and therefore facilitated the formation of hydrophobic microdomains. The I_3/I_1 values of copolymer **A** are quite different from those of copolymer **B** above their critical association temperatures (CATs). Obviously, the grafting density of PNIPAAm is rather important in regulating the structural response of the micelle-like polymeric aggregates to changes in temperature. The ionized PAAc backbone with very strong hydrophilicity and PEG grafts that had a LCST value (>70 °C) much higher than the transition temperature (32−34 °C) were insensitive to changes in temperature, and therefore, they did not contribute to the enhanced hydrophobicity of the copolymers to an appreciable extent in the range of temperature investigated. It is noteworthy that the I_3/I_1 values of the copolymers upon their abrupt conformational change with increasing temperature are lower than the usual I_3/I_1 values obtained from the micelle formation of surfactants, such as sodium dodecyl sulfate (ca. 0.82). This implies that the polymeric aggregates exhibit a quite different particle morphology compared to the conventional micelles comprising small surfactant species. Above the CAT, although the I_3/I_1 value of pyrene gradually increased with increasing temperature, the fluorescence data alone are still insufficient to justify the formation of hydrophobic PNIPAAm microdomains within polymeric aggregates due to the inherent effect of temperature on the pyrene fluorescence emission.[26]

In response to the hydrophobic association of the copolymers as illustrated in Figure 2, the hydrodynamic diameter of polymeric aggregates (D_h) changed dramatically (Figure 3). As the temperature increased from 25 to 35 °C, the formation of aggregates with remarkable hydrodynamic sizes was observed. The maximal D_h values were achieved in the range 34−35 °C. Beyond the CATs, the particle sizes were reduced significantly. Undoubtedly, the initial formation of aggregates was induced thermally by the extensive intermolecular hydrophobic interaction among the PNIPAAm grafts. At this initial stage, especially in the range 34−35 °C, the difference in the degree of intermolecular association and therefore the hydrodynamic sizes of the aggregates between copolymers **A** and **B** resulted from the different local PNIPAAm concentrations. Because of the thermally induced amphiphilic characteristic of the copolymers with increasing temperature, the polymer chains spontaneously rearranged themselves into micelle-like aggregates with either mono- or multicore structure. Studies on the micelle structure primarily based on the particle size data in this regard were reported in the literature.[17,18] However, to achieve an appropriate hydrophilic/hydrophobic balance, the negatively charged PAAc backbone as the shell of polymeric micelles associated with the hydrophobic PNIPAAm core may lead to large particles with the monocore structure. It is thus necessary to justify the micelle formation mechanism prior to the evaluation of the changed micelle structure with temperature.

Above 35 °C, the particle size decreased rapidly with increasing temperature (Figure 3). In addition, the size of polymeric micelles **B** became significantly smaller than that of micelles **A** in the range 35−60 °C. Such a size reduction was postulated to be thermally driven by either fragmentation of polymeric aggregates or dehydration of the hydrophobic core. However, shrinkage of the hydrophobic core, although occurring more profoundly in the single-core structured micelles, usually leads to a rather limited decrease in particle size. More importantly, on the basis of the single-core model, micelles **B** with initially larger sizes presumably due to the higher PNIPAAm concentration and therefore the larger hydrophobic core seem unlikely to transform into smaller particles than micelles **A** simply by the thermal reduction of the core size. On the other hand, fragmentation of polymeric micelles with the multicore structure can result from the partial breakage of connections among the hydrophobic cores within the large aggregates. Therefore, the particle size was significantly reduced, and the final particle size was dependent on the extent of the breakage in the intercore connections.

Further evidence in supporting the multicore micelle structure was provided by the further decreased particle size after mild agitation of the colloidal system at each preset temperature, as shown in Figure 4. This is because the shear force also partially destroyed the intercore connections within polymeric aggregates, thereby leading to the further fragmentation and decrease in the particle size. While the particle size of micelles **B** was reduced by agitation more profoundly

than that of micelles **A** in the range 32−35 °C, little effect of agitation was observed with the temperature being increased from 35 to 60 °C. These results rationalize our hypothesis that the multicore structure formed as a consequence of the intercore chain associations in the range 32−35 °C. Nevertheless, the rather weak connections were vulnerable to heating and shear force. The AAc residues in the backbone were in the charged state, and thus, the hydrophobic cores in a polymeric aggregate were connected to each other only via the interaction between PEG and PNIPAAm grafts. Individual cores formed simultaneously in part by association of the different PNIPAAm grafts attached to the same macromolecule. The PAAc main chains present in the hydrophilic outer layers of micelles acted as a bridging role since their PNIPAAm grafts took part in different hydrophobic core regions during the micelle formation period. This bridging effect then led to a strong connection among the hydrophobic cores within an aggregate. The electrostatic repulsion force among the ionized AAc residues made the backbone more extended in the aqueous phase, and this might also promote the formation of the multicore structure. Similarly, in the same temperature range, the interactions of the intramolecular PEG grafts with different hydrophobic PNIPAAm cores within an aggregate induced the second type of the intercore connections. With a preset temperature interval of 1 °C for 30 min from 32 to 35 °C, the thermally associative PNIPAAm cores formed with somewhat loose, and hydrated structure and their interactions with the PEG grafts reached maxima at ca. 35 °C (virtually at 34 °C for copolymer **B**). However, this kind of connection involving PEG grafts was more labile, and it was responsible mostly for the reduced particle size with further temperature increase and agitation (if present). Scheme 2 illustrates locally the fragmentation of the polymeric aggregate into smaller particles by partially destroying the intercore PEG connections when temperature increases.

Following the proposed hypothesis, the significant difference in particle size between micelles **A** and **B** in the phase transition temperature range was primarily due to the varying extents of the interaction of the PEG grafts with the hydrophobic PNIPAAm regions within the polymeric aggregates. The concentration of PNIPAAm grafts played a key role in governing the interaction between PNIPAAm and PEG grafts. Therefore, a more pronounced effect of agitation was observed for copolymer **B** in the range 32−35 °C. Further increasing the temperature above the CATs, the PNIPAAm cores were continually dehydrated and showed weaker tendency to interact with PEG grafts. Owing to the higher local PNIPAAm concentration accompanied by the greatly enhanced hydrophobicity, micelles **B** were thus fractured into smaller particles in this temperature range as compared to micelles **A**. Furthermore, the thermally induced extensive breakage of the PEG connections within micelles **B** renders agitation less effective in reducing particle size. Nevertheless, the multicore structure of micelles still maintained in an aggregate form as a consequence of the intact PNIPAAm bridging among the hydrophobic cores.

It should be noted that the above hypothesis is only valid based on the following assumptions. First, the core structure of polymeric micelles continually changes with temperature even above the CATs. Second, changes in the interaction of the PEG grafts with hydrophobic cores

Scheme 2. Local Illustration of the Structure of Polymeric Aggregates in the Range 32−35 °C and the Structural Change with Further Increasing Temperature[a]

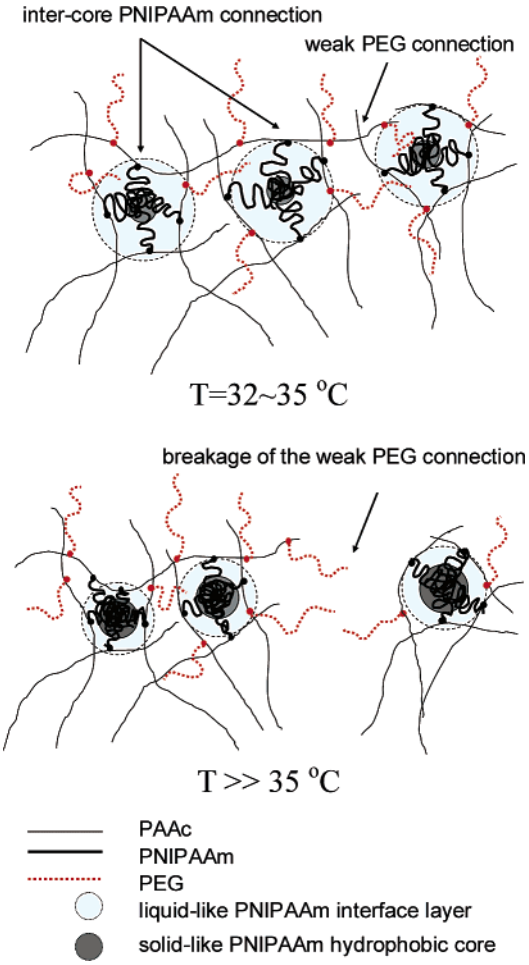

[a] The fragmentation of the aggregates occurs owing to the breakage of the weak PEG connections among the hydrophobic cores while the dehydration of the liquidlike PNIPAAm interfacial layers proceeds with increasing temperature.

are primarily governed by the core structure, which solely depends on the PNIPAAm concentration and temperature. In addition, fragmentation of the aggregates occurs as a result of the thermally reduced interaction of the PEG grafts with the hydrophobic PNIPAAm cores within micelles.

Figure 5 illustrates the typical ^{1}H NMR spectra of copolymer **B** in D_2O at various temperatures. The feature signal of DMF as an external standard in the NMR measurements at δ 8.1 ppm was selected as the reference resonance in the spectrum analysis. The chemical shift of DMF at 8.1 ppm was predetermined on the basis of the reference line of DHO at 4.8 ppm at 20 °C. DHO was not chosen since the feature signal of DHO became upfield shifted with increasing temperature as it was also reported elsewhere.[27] Figure 5 shows that while the chemical shift of the methyl protons of PNIPAAm grafts at δ 1.1 ppm is rather invariant, its integral decreased significantly with increasing temperature. It is now generally recognized that, owing to the distinct difference in the mobility of hydrophobic segments in the core region, micelles can be created with either liquid- or solidlike core structure. The solidlike core formation was usually characterized in the liquid ^{1}H NMR measurements by the fast and dramatic

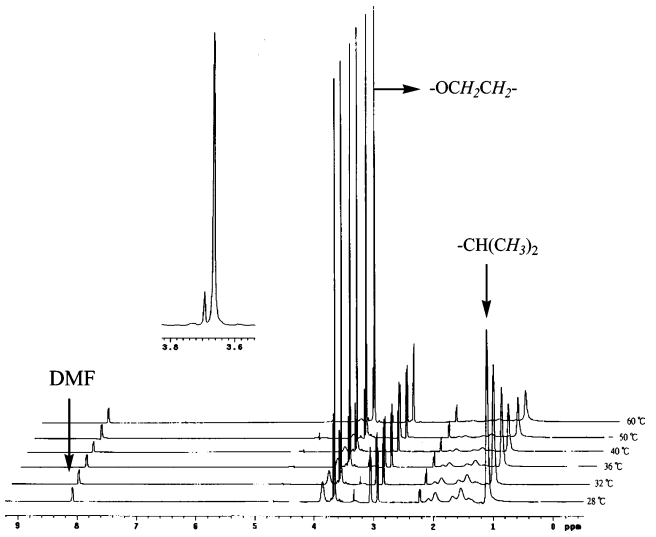

Figure 5. ^{1}H NMR spectra of copolymer **B** (10.0 mg/mL) in D_2O at different temperature. The inset represents the feature proton signals of the mPEG grafts of copolymer **B** at 36 °C.

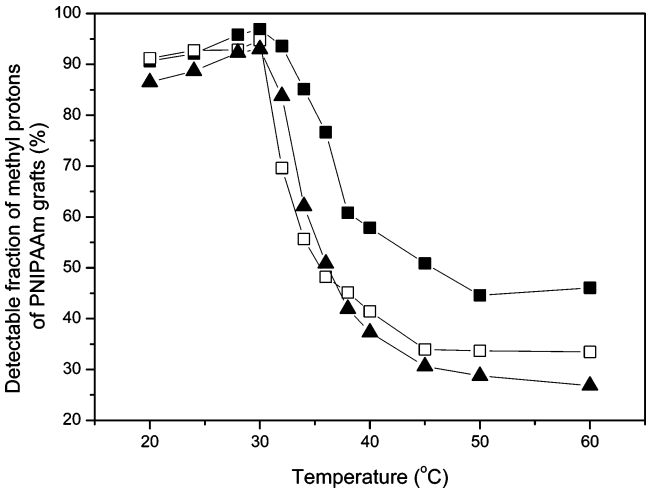

Figure 6. Detectable fraction (%) of the methyl protons (1.1 ppm) of the PNIPAAm grafts of copolymer **A** (■) 10.0 and (▲) 30.0 mg/mL) and copolymer **B** (□) (10.0 mg/mL) in D_2O in ^{1}H NMR measurements as a function of temperature with respect to its signal integral in $CDCl_3$ at 20 °C, using the DMF signal at 8.1 ppm as a reference.

decrease in the spin−lattice relaxation time (T_1), rendering the corresponding proton signals undetectable. Above the CATs, the colloidal system was gradually transformed into the more solidlike core structure when temperature increased. It should be noted that the methyl proton signals did not fully disappear even at 60 °C, in contrast to the entire disappearance of the same proton signal for the homopolymer PNIPAAm at 35 °C.[28] Although splitting mainly into two peaks, the feature signal integral from the ethylene protons of PEG grafts with respect to the DMF standard signal remained constant with increasing temperature and was essentially identical to that measured in $CDCl_3$ (Figure 1). The proton signal that was originally downfield shifted at room temperature comparing to that in $CDCl_3$ (from 3.60 ppm in $CDCl_3$ to 3.66 ppm in D_2O) became slightly upfiled shifted with increasing temperature due to partial breakage of the hydrogen bonds with D_2O molecules. Nevertheless, the results of the constant peak integral with temperature indicate that PEG grafts within micelles barely interacted with or embedded in the solidlike core regions even though the latter increased with increasing temperature.

The fractions of the liquidlike structure in hydrophobic microdomains in terms of the detectable PNIPAAm fractions in the ^{1}H NMR measurements for copolymers **A** and **B** as a function of temperature are shown in Figure 6. It is noteworthy that the detectable fractions in Figure 6 were somewhat overestimated due to the stronger interaction of the copolymers with D_2O than with H_2O molecules.[16] In the micelle formation, the core structure was developed in the form of both solid- and liquidlike structure. On the basis of the significant PNIPAAm fractions detected, the liquidlike hydrophobic regions exist most probably at the interface between the solidlike cores and hydrophilic shells full of the negatively charged PAAc segments. Moreover, the liquidlike interface occurred as a result of the hydration of PNIPAAm grafts and their interactions with PEG grafts. The liquidlike interfacial region was gradually dehydrated and solidified with increasing temperature, thereby leading to the decrease of its interaction with PEG grafts and, more importantly, the fragmentation of polymeric aggregates. Apparently, because of the higher local concentration of the PNIPAAm grafts of copolymer **B** than that of copolymer **A**, the higher ratio of the solid/liquidlike core structure in micelles **B** was obtained (Figure 6). Thus, a more significant reduction in the PEG connections and in particle size of micelles **B** at high temperature was achieved (Figure 3). The observation of the maximal detectable fractions of PNIPAAm of the copolymers at the temperature just prior to the CATs in Figure 6 was also similarly reported elsewhere.[29,30] It was explained by the formation of extensive hydrogen bonds between the NIPAAm residues and water molecules at this temperature via the FTIR-ATR measurements.[30] The effect of the polymer concentration (10 and 30 mg/mL of copolymer **A**) on the resultant core structure as shown in Figure 6 will be discussed below.

The response in the segmental mobility of PNIPAAm (in the liquidlike interface) and PEG grafts to the changed core structure with increasing temperature was evaluated by the proton spin−lattice relaxation time (T_1) measurements. Figure 7A shows the Arrhenius plots of the T_1 values from two feature signals (the methyl and methyne protons of the isopropyls) of PNIPAAm grafts in the liquidlike interface. The T_1 values of both the methyne and methyl groups of isopropyls increased with increasing temperature. Owing to the relation of T_1 with the correlation time τ as usually described by the BPP theory and the dependence of τ on temperature in the Arrhenius manner, a minimum of T_1 is usually found for a specific proton in the plot of T_1 against temperature.[31,32] Therefore, with respect to the temperature at the minimum, the T_1 temperature curve can usually be divided into high- and low-temperature phases. The location of the curve in either phase is primarily governed by the product of Lamor frequency and correlation time.[32] Because of the fixed Lamor frequency in this study and relatively high thermal mobility of the isopropyl groups, the T_1 values fell into the high-temperature phase and increased with increasing temperature. Upon the micelle formation, the inherent increased rates of T_1 for the isopropyl (methyne and methyl) protons of PNIPAAm graft with temperature are anticipated to be reduced, owing to a decrease in their mobility by the hydrophobic aggregation. A significant change in the T_1 temperature curve of the

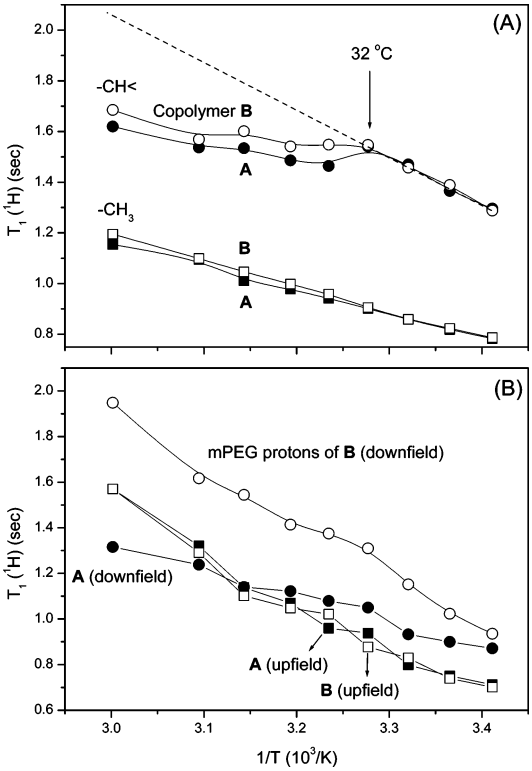

Figure 7. Temperature dependence of the spin−lattice relaxation times (T_1) of (A) the methyne and methyl protons of isopropyls from PNIPAAm grafts in copolymers **A** and **B** in D_2O (10.0 mg/mL) and (B) of the upfield and downfield mPEG protons (shown in the inset of Figure 5) of the two copolymers.

methyne protons just above 32 °C was observed in accordance with this assumption. Unlike a dramatic decrease in T_1 for the methyne proton of linear homo-PNIPAAm upon the phase transition, the T_1 values herein kept increasing with increasing temperature, indicating a looser and more heterogeneous structure of the liquidlike PNIPAAm interlayer. The T_1 of the methyne protons of micelles **A** was slightly lower than that of micelles **B** at elevated temperature. This is attributed to the structural difference in the liquidlike interfacial layers between micelles **A** and **B**. More extensive interaction of the liquidlike interface of micelles **A**, primarily in the amide linkages, with PEG grafts resulted in more hydration. Both the higher extents of hydration and interaction with PEG of the liquid like interface of micelles **A** enhanced the intermolecular dipole−dipole relaxation and the magnetogyric ratio of the proton and thus shortened its T_1.[33] However, the structural distance between the methyl group and the amide linkage allows only a slight difference in T_1 for the methyl protons between micelles **A** and **B**. The T_1 temperature curve for the methyl protons of PNIPAAm grafts was also affected insignificantly by the micelle formation due to the higher rotational energy.

Owing to the different chemical environments of PEG grafts, two feature signals of the ethylene protons were observed, as shown in the inset of Figure 5. The upfield signal was identical in the chemical shift to that of the ethylene protons of free mPEG in D_2O and assigned to the fully mobile PEG grafts locating outside of the micelle structure. Primarily because of the inductive effect of the surroundings full of the negatively charged PAAc main chains, most of the PEG grafts residing within polymeric micelles appeared downfield shifted

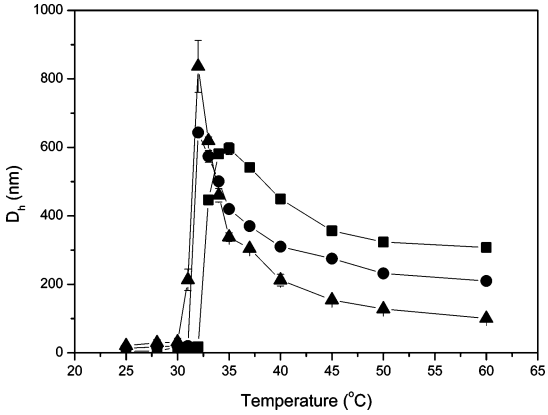

Figure 8. Variation of the *z*-average hydrodynamic diameter (D_h) of copolymer **A** with the concentrations of (■) 10.0, (●) 20.0, and (▲) 30.0 mg/mL in aqueous solutions with temperature in the absence of agitation.

by deshielding their protons in the applied magnetic field. As expected, these characteristic double signals disappeared at pH 3.0, where the AAc residues remained mostly in the uncharged state. The T_1 values of the upfield mPEG signals for micelles **A** and **B** at different temperature were thus essentially identical, as shown in Figure 7B. Little effect of the micelle formation on T_1 was also observed. In contrast, significantly different T_1 values for the downfield protons between micelles **A** and **B** were obtained. In micelles **A**, the PEG grafts within micelles interacted more extensively with PNIPAAm grafts in the liquidlike interface, and therefore, T_1 was shortened due to the much more restricted mobility.

As aforementioned, changes in the core structure and particle size of polymeric micelles with increasing temperature were virtually controlled by the concentration of PNIPAAm grafts. The effect of the PNIPAAm concentration on particle size is demonstrated by changing the graft copolymer concentration, as shown in Figure 8. The results indicate that aggregates with large size formed with more extensive PEG bridging by increasing the PNIPAAm concentration in the range 32−35 °C. It is also interesting to note that the sizes of micelles **A** at 30 mg/mL were approximately the same as those of micelles **B** at 10 mg/mL in the range from 35 to 60 °C (by comparing Figures 3 and 8). Although the PNIPAAm concentration was 2.2 times lower than that of copolymer **A** at 30 mg/mL, copolymer **B** (10 mg/mL) undoubtedly exhibited a more effective local concentration of PNIPAAm in the core formation. Notably, the results of the detectable PNIPAAm fractions in Figure 6 were in good agreement with the particle size data. Micelles **A** at 30 mg/mL showed similar core structures, i.e., the similar ratios of the solid/liquidlike hydrophobic regions, to micelles **B** at 10 mg/mL. This confirms our hypothesis that the particle size of this colloidal system above the CATs (Figures 3 and 8) was primarily determined by the response of the core structure to the temperature increase via the enhanced hydrophobic effect on partially breaking the PEG connections and fracturing the polymeric aggregates.

It is noteworthy that the entire micelle structure can be additionally influenced by the interaction of polymeric micelles with water molecules while the dehydration of the hydrophobic cores continues to proceed with increasing temperature. The interaction of the copolymer with water molecules was studied in terms of

changes in the volume (or density) of the graft copolymers in aqueous solution with temperature.[34] For comparison purposes, the dependence of the apparent densities of mPEG and PNIPAAm in water on temperature was also evaluated. The results (data not shown here) indicates that the apparent density of mPEG in aqueous solution decreased linearly with increasing temperature in the entire range investigated (coefficient of determination $R = 0.9999$). The decrease in the density of mPEG was obviously due to the increased partial volume as a result of the thermal expansion and alteration in its interaction with water. Similarly, the linear dependence of the apparent densities on temperature ($R = 0.9990$) was obtained for PNIPAAm and the graft copolymers in the range 20−28 °C. However, because of the phase transition of the copolymers and continual dehydration of the hydrophobic cores in micelles, the increased deviation of density from the linear relationship with temperature occurred. Since the degree of the deviation (δ) represents a quantitative measure of the variation in the interaction between polymeric micelles and water molecules with respect to their presumable interaction in the absence of the polymer phase transition, an interaction function, $f(\delta)$, that becomes unity at low temperature (20−28 °C) can be defined as follows:

$$f(\delta) \equiv \rho_m(T)/\rho_t(T) \tag{3}$$

where $\rho_m(T)$ is the polymer density measured by densimeter and $\rho_t(T)$ the theoretical density obtained from the extrapolation of the linear relationship in the absence of the phase transition. Notably, because of the existence of the linear relationship as aforementioned, the deviation of the volume of the polymer aqueous solution from the volume additivity assumption was mostly self-corrected in obtaining the interaction parameter from eq 3.

The temperature dependence of $f(\delta)$ of mPEG and PNIPAAm homopolymers and of copolymers **A** and **B** with various concentrations is shown in parts A and B of Figure 9, respectively. As expected, this interaction parameter between mPEG and water molecules kept independent of temperature at 1.0, owing to the absence of the phase transition in the temperature range employed. In agreement with the ^{1}H NMR data, the interaction of PNIPAAm and its graft copolymers with water molecules reached a maximum just prior to the phase transition temperatures. Since the difference in $f(\delta)$ signifies the different interactions of polymeric micelles with water molecules, Figure 9B remarkably demonstrates only a slight effect of the polymer concentration (10−30 mg/mL) on the interaction of micelles with water molecules. Owing to the concomitant increased concentrations of the PAAc main chains and mPEG grafts with increasing the polymer concentration, the interaction of hydrophilic polymeric segments with water molecules inevitably increased, thereby leading to a balanced contribution against the increased dehydration of hydrophobic cores. On the other hand, because of the difference in the concentrations of polar and hydrophilic polymeric segments, significant differences in the interaction of macromolecules with water molecules were observed between micelles **B** of 10 mg/mL and **A** of 30 mg/mL even though the hydrophobic core structures of these two colloidal systems were quite similar (Figure 6). Therefore, these results strongly support our hypothesis that the particle size is virtually

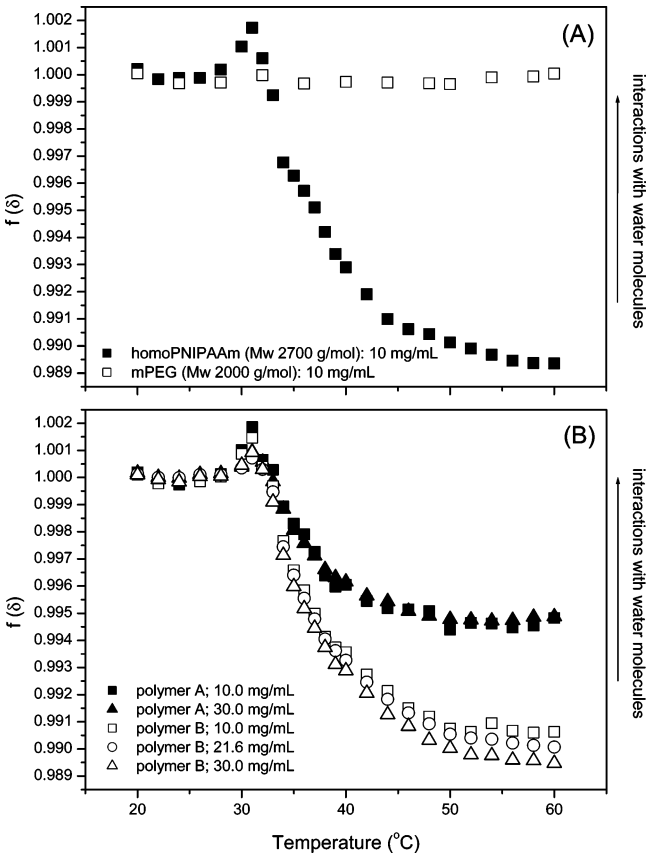

Figure 9. Temperature dependence of the function of deviation in the interaction of macromolecules with water molecules of (A) PNIPAAm and mPEG homopolymers and (B) copolymers **A** and **B** with different concentrations in aqueous solutions. The PNIPAAm concentration of copolymer **A** at 30.0 mg/mL is equal to that of copolymer B at 21.6 mg/mL.

governed by the structure of the hydrophobic core regions of micelles via the fragmentation process, irrespective of the concentrations of polar and hydrophilic polymeric segments and their interactions with water molecules.

Conclusion

In this study, graft copolymers comprising monomeric units of AAc as the backbone and PNIPAAm and mPEG, as the grafts were prepared by partial aminolysis of PNAS with aminated semitelechelic PNIPAAm and mPEG, followed by thorough hydrolysis of the remaining NAS residues to AAc units. The supramolecular structure of the graft copolymers in the aqueous phase above the CATs was characterized. Large polymeric aggregates (D_h > 600 nm) were observed in the temperature range in which phase separation occurred due to the formation of the multicore structure within polymeric aggregates and the extensive interaction of PEG grafts with PNIPAAm grafts present in the hydrophobic liquidlike interfacial regions. However, this interaction decreased with further thermal dehydration and solidification of the liquidlike PNIPAAm interface, thereby leading to fragmentation of polymeric aggregates into smaller particles with the more distinct core/shell structure. The varied proton spin−lattice relaxation time (T_1) of the mPEG grafts within micelles with the PNIPAAm concentration also confirms the strong dependence of the interaction between PEG and PNIPAAAm grafts on the structure (i.e., the ratio of the

solid/liquidlike regions) of the hydrophobic cores. Therefore, the particle size was primarily controlled by the structural response of the hydrophobic regions to changes in the PNIPAAm concentration and temperature through the breakage of the PEG connections among the core regions within micelles, irrespective of the interactions of the polar and hydrophilic polymeric segments with water molecules.

Acknowledgment. This work was supported by the National Science Council of Taiwan (NSC92-2218-E-005-002).

References and Notes

(1) Hrkach, J. S.; Peracchia, M. T.; Domb, A.; Lotan, N.; Langer, R. *Biomaterials* **1997**, *18*, 27.
(2) Heald, C. R.; Stolnik, S.; Kujawinski, K. S.; De Matteis, C.; Garnett, M. C.; Illum, L.; Davis, S. S.; Purkiss, S. C.; Barlow, R. J.; Gellert, P. R. *Langmuir* **2002**, *18*, 3669.
(3) Chang, Y.; Bender, J. D.; Phelps, M. V. B.; Allcock, H. R. *Biomacromolecules* **2002**, *3*, 1364.
(4) Yamamoto, Y.; Yasugi, K.; Harada, A.; Nagasaki, Y.; Kataoka, K. *J. Controlled Release* **2002**, *82*, 359.
(5) Minatti, E.; Viville, P.; Borsali, R.; Schappacher, M.; Deffieux, A.; Lazzaroni, R. *Macromolecules* **2003**, *36*, 4125.
(6) Ma, Y.; Cao, T.; Webber, S. E. *Macromolecules* **1998**, *31*, 1773.
(7) Gohy, J.-F.; Hofmeier, H.; Alexeev, A.; Schubert, U. S. *Macromol. Chem. Phys.* **2003**, *204*, 1524.
(8) Chiu, H. C.; Hu, C. H.; Chern, C. S. *Polym. J.* **1999**, *31*, 535.
(9) Konak, C.; Reschel, T.; Oupicky, D.; Ulbrich, K. *Langmuir* **2002**, *18*, 8217.
(10) Virtanen, J.; Tenhu, H. *Macromolecules* **2000**, *33*, 5970.
(11) Virtanen, J.; Lemmetyinen, H.; Tenhu, H. *Polymer* **2001**, *42*, 9487.
(12) Virtanen, J.; Holappa, S.; Lemmetyinen, H.; Tenhu, H. *Macromolecules* **2002**, *35*, 4763.
(13) Durand, A.; Hourdet, D. *Polymer* **1999**, *40*, 4941.
(14) Barbier, V.; Herve, M.; Sudor, J.; Brulet, A.; Hourdet, D.; Viovy, J. L. *Macromolecules* **2004**, *37*, 5682.
(15) Neradovic, D.; Soga, O.; Van Nostrum, C. F.; Hennink, W. E. *Biomaterials* **2004**, *25*, 2409.
(16) Maeda, Y.; Taniguchi, N.; Ikeda, I. *Macromol. Rapid Commun.* **2001**, *22*, 1390.
(17) Schilli, C. M.; Zhang, M.; Rizzardo, E.; Thang, S. H.; Chong, Y. K.; Edwards, K.; Karlsson, G.; Muller, A. H. E. *Macromolecules* **2004**, *37*, 7861.
(18) Yusa, S.; Shimada, Y.; Mitsukami, Y.; Yamamoto, T.; Morishima, Y. *Macromolecules* **2004**, *37*, 7507.
(19) Qiu, X.; Wu, C. *Macromolecules* **1997**, *30*, 7921.
(20) Qiu, X.; Kwan, C. M. S.; Wu, C. *Macromolecules* **1997**, *30*, 6090.
(21) Adalsteinsson, O.; Lamotte, A.; Baddour, R. F.; Colton, C. K.; Pollak, A.; Whitesides, G. M. *J. Mol. Catal.* **1979**, *6*, 199.
(22) Chen, G.; Hoffman, A. S. *Nature (London)* **1995**, *373*, 49.
(23) Zalipsky, S.; Gilon, C.; Zilkha, A. *Eur. Polym. J.* **1983**, *19*, 1177.
(24) Kalyanasundaram, K.; Thomas, J. K. *J. Am. Chem. Soc.* **1977**, *99*, 2039.
(25) McConville, P.; Whittaker, M. K.; Pope, J. M. *Macromolecules* **2002**, *35*, 6961.
(26) Winnik, F. M. *J. Phys. Chem.* **1989**, *93*, 7452.
(27) Gottlieb, H. E.; Kotlyar, V.; Nudelman, A. *J. Org. Chem.* **1997**, *62*, 7512.
(28) Zeng, F.; Tong, Z.; Feng, H. *Polymer* **1997**, *38*, 5539.
(29) Zhu, P. W.; Napper, D. H. *Colloids Surf. A* **1996**, *113*, 145.
(30) Lin, S. Y.; Chen, K. S.; Liang, R. C. *Polymer* **1999**, *40*, 2619.
(31) Bloembergen, N.; Purcell, E. M.; Pound, R. V. *Phys. Rev.* **1948**, *73*, 679.
(32) Tokuhiro, T.; Amiya, T.; Mamada, A.; Tanaka, T. *Macromolecules* **1991**, *24*, 2936.
(33) Podo, F.; Ray, A.; Nemethy, G. *J. Am. Chem. Soc.* **1973**, *95*, 6164.
(34) Zafarani-Moattar, M. T.; Mehrdad, A. *J. Chem. Eng. Data* **2000**, *45*, 386.

MA0512713